Enhanced resilience towards ROADM-induced optical filtering using subcarrier multiplexing and optimized bit and power loading

Research Article | Vol. 27, No. 21 / 14 October 2019 / Optics Express 30710
Optics EXPRESS

Enhanced resilience towards ROADM-induced optical filtering using subcarrier multiplexing and optimized bit and power loading

A. M. Rosa Brusin,[1] F. P. Guiomar,[2,*] A. Lorences-Riesgo,[2] P. P. Monteiro,[2,3] and A. Carena[1]

[1] *Dipartimento di Elettronica e Telecomunicazioni, Politecnico di Torino, Corso Duca degli Abruzzi, 24, 10129 Torino, Italy*
[2] *Instituto de Telecomunicações, Aveiro, Portugal*
[3] *Department of Eletronics, Telecommunications and Informatics, University of Aveiro, Portugal*
[*] *guiomar@av.it.pt*

Abstract: In flexible optical networks, lightpaths are routed from source to destination thanks to reconfigurable optical add-drop multiplexers (ROADMs) placed in every node connected by a line system. As ROADMs are based on wavelength selective switches (WSSs), which imply channel filtering, a non negligible performance reduction can be observed when lightpaths traverse many network nodes. Control plane software network controllers that base their decision on the quality of transmission of the physical layer must also take into account the impact of ROADMs cascading. The penalties caused by WSS cascading in single-carrier systems are mostly driven by uncompensated inter-symbol interference (ISI), and therefore their evaluation cannot be based on simple analytical solutions as required for real-time network control. In this paper, we consider a 200G optical system based on multi-subcarrier (MSC) modulation with hybrid modulation formats. Using a fully analytical framework, we show that it is possible to predict ROADM-induced penalties offline and accurately estimate the required settings for their transmitter-side mitigation through bit and/or power-loading. Moreover, resorting to both simulations and experiments, we also demonstrate that properly optimized MSC signals can provide an increased resilience to ROADM filtering with respect to standard single-carrier systems: applying analytically-driven bit-loading over 8×4 Gbaud and 16×2 Gbaud MSC signals after crossing 8 cascaded WSSs in a noise loading scenario, we experimentally found ~2 dB gain in required SNR with respect to a traditional 32 Gbaud single-carrier signal.

1. Introduction

The expected rapid increase of Internet data traffic in the next few years, mostly driven by the upcoming 5G communications along with its requirements and applications [1], will impose the use of flexible and high capacity optical networks. Dynamic flexibility of such networks can be provided by employing reconfigurable optical add-drop multiplexers (ROADMs) in the optical nodes. ROADMs are enabled by wavelength selective switches (WSSs), which perform channel routing on a wavelength basis allowing to dynamically set lightpaths in the network. To maximize the usage of the entire available bandwidth, i.e. to increase the spectral efficiency (SE), channels are shaped to limit their bandwidth occupation and the flex-grid concept is applied with very tight inter-channel spacing. As a consequence, the inter-symbol interference (ISI) induced by filtering effects increases, becoming more severe when the signal has to pass over several cascaded ROADMs, which significantly narrows the overall optical transfer function, and thereby degrades the quality of the received signal. This phenomenon is expected to become increasingly more detrimental in the near future, with a significant impact on mesh and long-haul networks, as illustrated in [2] where 75 GHz wide filters are considered for 62 and 67 GBaud carriers and in

#373545 https://doi.org/10.1364/OE.27.030710
Journal © 2019 Received 23 Jul 2019; revised 7 Sep 2019; accepted 8 Sep 2019; published 9 Oct 2019

Optics EXPRESS

[3] where the impact on probabilistic shaping is analyzed. For this reason, several solutions have been proposed to partially compensate for this penalty [4,5]. In [6] an adaptive compensation is proposed consisting in the adjustment of the tap coefficients of the finite impulse response (FIR) filter at the receiver.

The implementation of high capacity optical channels can be based on two different modulation approaches: single-carrier or multi-subcarrier (MSC). As an alternative to the widely used single-carrier modulation, it has been demonstrated that MSC signals, obtained through electronic subcarrier multiplexing (SCM), are more resilient to non-linear fiber effects, because they allow to operate close to the optimal symbol rate [7,8].

A recent long-haul experiment has shown the potentiality of using MSC in submarine transmissions, reaching 10,500 km with 4.66 b/s/Hz SE [9]. In addition to the enhanced non-linear robustness, we have also recently shown that MSC systems can also be more robust against the strong optical filtering caused by several cascaded WSSs [10]: in particular, a special flavor of MSC, using frequency-domain hybrid modulation formats (FDHMF), allows to choose the best modulation format of the type 2^N-QAM for each subcarrier (SC), thereby minimizing the impact of filtering effects. This paper extends the work presented in [10]. First, introducing the detailed theory developed to study the impact of ROADM filtering on hybrid MSC channels. Then, considering a comprehensive analysis of different cases. In [10] only an 8×4 GBaud MSC signal was compared to a 32 GBaud single-carrier one: here, keeping the overall 32 GBaud symbol rate fixed, we sweep the SC symbol rate (16, 8 and 2 GBaud), which corresponds to different number of SCs (respectively 2, 4 and 16). Moreover, we also consider a more realistic distributed noise insertion compared to the lumped noise case presented in [10].

Similarly to other previous works [11–13], we exploit and compare several FDHMF optimization strategies, which are known to reduce the impact of ROADM-induced filtering: bit-loading (BL), power-loading (PL) and bit-and-power-loading (BPL) [14]. BL consists in finding the best modulation format, per SC in our case, which reduces penalties without changing the transmitted power, PL adjusts the transmitted power (per SC) without changing the modulation format and BPL is the combination of BL and PL. However, as opposed to previous research works on this topic, we demonstrate for the first time that BL, PL and BPL can be accurately designed by a simple fully analytic framework, requiring only the knowledge of the characteristics of ROADMs cascaded along the optical link. This approach enables to offline predict the penalties caused by strong optical filtering and quasi-optimally design the best FDHMF configuration at the transmitter that maximizes performances without the need for a feedback channel from the receiver. Using the proposed ROADM filtering model for MSC modulation we experimentally demonstrate ~2 dB of SNR gain over single-carrier modulation at 32 GBaud, for a fixed 200G net bit-rate. Remarkably, we also find that the best filtering tolerance provided by MSC is obtained at symbol-rates per subcarrier that coincide with the optimum symbol-rates required for minimal nonlinear interference, which is an important result for system design in metro and long-haul optical networks.

The remaining of this paper is organized as follows. After introducing the theoretical background in Section 2, in Section 3 we optimize the number of SCs through simulations. Then, in Section 4, we provide an experimental validation using the same setup presented in [10]. Section 5 is dedicated to conclusions.

2. Theoretical background

The WSS optical transfer function is often addressed in the literature through the fitting of super-Gaussian functions of variable order [15]. Alternatively, a physical model of WSS filtering has been proposed in [16], where the band-pass spectral response is given by the convolution between the WSS rectangular aperture bandwidth B and the bandwidth of the Gaussian shaped optical transfer function (OTF) B_{OTF}, which is the -3 dB bandwidth. Defining the standard

Optics EXPRESS

deviation as $\sigma = B_{\text{OTF}}/\left(2\sqrt{2\log 2}\right)$, the overall normalized transfer function is given by

$$S(f) = \left[\frac{1}{2}\text{erf}\left(\frac{B/2-f}{\sqrt{2}\sigma}\right) - \frac{1}{2}\text{erf}\left(\frac{-B/2-f}{\sqrt{2}\sigma}\right)\right]^{N_{\text{WSS}}}, \tag{1}$$

where $\text{erf}(x) = \frac{2}{\sqrt{\pi}}\int_0^x \exp\left(-x^2\right) dx$ is the error function, B is the bandwidth of the frequency slot in which the WSS is placed and N_{WSS} is the number of cascaded WSSs. In this paper we consider $B = 37.5$ GHz, $B_{\text{OTF}} = 10.4$ GHz and $N_{\text{WSS}} \in \{0, \ldots, 8\}$ that corresponds to cascading up to 4 ROADMs, as usually one ROADM requires the signal to go through 2 WSS filters [15]. An example of the effect of 8 cascaded WSSs on an MSC signal composed of 8×4 GBaud subcarriers is shown in Fig. 1(a): as expected, filtering effects are stronger in the edge subcarriers.

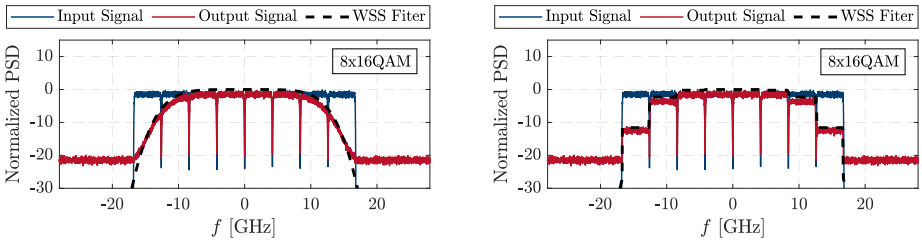

(a) Real WSS filtering (b) Approximated WSS filtering

Fig. 1. Effects of the transfer functions of (a) a real WSS filter and of (b) the zeroth-order approximated WSS filter on an 8×4 GBaud MSC input signal after 8 cascaded WSSs.

To simplify the theoretical analysis, we introduce a zeroth-order approximation of the WSS filter in the frequency-domain, which basically corresponds to polynomial fitting of degree 0, i.e. a flat attenuation within each subcarrier bandwidth corresponding to its average power loss, $\hat{L}_{\text{SC}_n}$, that impacts every subcarrier when passing through N_{WSS} WSSs,

$$\hat{L}_{\text{SC}_n} = \int_{f_{\text{SC}_n}-\frac{R_s}{2}(1+\alpha)}^{f_{\text{SC}_n}+\frac{R_s}{2}(1+\alpha)} \left|S(f)\cdot p(f-f_{\text{SC}_n})\right|^2 df, \tag{2}$$

where R_s is the symbol-rate of each subcarrier, α is the roll-off factor of the pulse shaping filter $p(f)$, whose energy is normalized to 1, and f_{SC_n} is the central frequency of subcarrier number n, which is set according to the minimum frequency spacing that avoids inter-subcarrier crosstalk,

$$f_{\text{SC}_n} = \left(n - \frac{N_{\text{SC}}+1}{2}\right)(1+\alpha)R_s, \tag{3}$$

where N_{SC} is the total number of subcarriers. Considering a standard root-raised cosine pulse shaping filter with α<0.1, we can assume a quasi-rectangular transfer function for $p(f)$. In that case, expression (2) can be simplified as,

$$\hat{L}_{\text{SC}_n} = \frac{1}{R_s}\int_{f_{\text{SC}_n}-\frac{R_s}{2}}^{f_{\text{SC}_n}+\frac{R_s}{2}} |S(f)|^2 df. \tag{4}$$

An example of the application of this zeroth-order approximation of the WSS transfer function is shown in Fig. 1(b), for the case of 8 cascaded WSSs and an 8×4 GBaud MSC signal. Making use of this average power loss per subcarrier, we can easily derive a *local* SNR for each subcarrier,

Optics EXPRESS

$\mathrm{SNR}_{\mathrm{SC}_n}$, from the *global* SNR of the entire multi-subcarrier signal, $\mathrm{SNR}_{\mathrm{MSC}}$,

$$\mathrm{SNR}_{\mathrm{SC}_n} = \mathrm{SNR}_{\mathrm{MSC}} - 10\log_{10}(\hat{L}_{\mathrm{SC}_n}) + \mathrm{PR}_{\mathrm{SC}_n}, \tag{5}$$

where $\mathrm{PR}_{\mathrm{SC}_n}$ is the power-ratio in dB between the n-th subcarrier, P_{SC_n}, and the average power of the entire MSC signal, defined as:

$$\mathrm{PR}_{\mathrm{SC}_n} = 10\log_{10}\left(N_{\mathrm{SC}}\frac{P_{\mathrm{SC}_n}}{\sum_{n=1}^{N_{\mathrm{SC}}} P_{\mathrm{SC}_n}}\right). \tag{6}$$

Under this assumption, it can be easily perceived that any inter-symbol interference (ISI) due to optical filtering effects is neglected, since only the SNR reduction due to the WSS-induced power loss is considered. By doing this, we ideally assume that any ISI can be completely compensated for at the receiver, resorting to digital signal processing. However, it is well known that realistic digital equalizers cannot ideally compensate for deterministic distortions (such as WSS-induced ISI) in scenarios with additive noise sources, due to the phenomenon of digital noise enhancement. Indeed, the noise enhancement caused by digital filtering at the receiver can be highly detrimental for single-carrier signals. Nevertheless, as the number of subcarriers is increased, the in-band distortion perceived by each subcarrier tends to become increasingly flat over frequency, thus requiring less or even no digital equalization, thereby circunventing the digital noise enhancement issue. In fact, for a fairly large number of subcarriers, the approximation of expression (2) will tend to converge to the exact solution, in which case the impact of WSS filtering suffered by each subcarrier effectively becomes a simple power loss, thus requiring no equalization at the receiver. The open question at this point, which we will try to clarify by extensive simulations and experiments in the following sections, is to find the minimum number of subcarriers that enables to achieve a good agreement between performance estimation based on this zeroth-order approximation and the real case. Another implicit assumption of expression (5) is that the WSS filtering only induces a power loss over each subcarrier without removing any added noise along the link. This is in fact a worst case assumption, which corresponds to a lumped insertion of ASE noise at the receiver side.

In addition to exploiting the inherent optical filtering mitigation provided by MSC signals, the main purpose of the proposed WSS approximation is to allow obtaining *a-priori* estimates of bit-error ratio (BER) for each subcarrier, $\mathrm{BER}_{\mathrm{SC}_n}$, using simple closed-form analytic formulas,

$$\mathrm{BER}_{\mathrm{SC}_n} = \Psi\left(\mathrm{SNR}_{\mathrm{SC}_n}, M_{\mathrm{SC}_n}\right), \tag{7}$$

where M_{SC_n} is the order of the M-QAM constellation corresponding to subcarrier number n, and $\Psi(\mathrm{SNR}_{\mathrm{SC}_n}, M_{\mathrm{SC}_n})$ is a nonlinear function that depends only on the SNR and modulation order, M, of each subcarrier. Note that both approximate and exact closed-form expressions for $\Psi(\cdot)$ are widely available in the literature [17,18].

Finally, by assuming a joint FEC encoder/decoder among all subcarriers, we can calculate the overall BER of the MSC signal simply as,

$$\mathrm{BER}_{\mathrm{MSC}}(\mathbf{SNR_{SC}}, \mathbf{M_{SC}}) = \frac{1}{\sum_{n=1}^{N_{\mathrm{SC}}}\log_2(M_{\mathrm{SC}_n})}\sum_{n=1}^{N_{\mathrm{SC}}}\Psi(\mathrm{SNR}_{\mathrm{SC}_n}, M_{\mathrm{SC}_n})\log_2(M_{\mathrm{SC}_n}), \tag{8}$$

where $\mathbf{SNR_{SC}}$ and $\mathbf{M_{SC}}$ are vectors with N_{SC} components, $\mathrm{SNR}_{\mathrm{SC}_n}$ and M_{SC_n}, respectively.

A block diagram depicting the integrated MSC optimization framework is shown in Fig. 2, where the upper part represents the required inputs that can typically be obtained from the control plane:

- parameters of the WSSs (B, B_{OTF} and N_{WSS}) that have been traversed by the signal;

Optics EXPRESS

- parameters of the MSC signal (f_{SC_n}, N_{SC}, $\mathbf{M_{SC}}$ and $\mathbf{PR_{SC}}$);
- estimated overall SNR of the MSC signal, SNR_{MSC}.

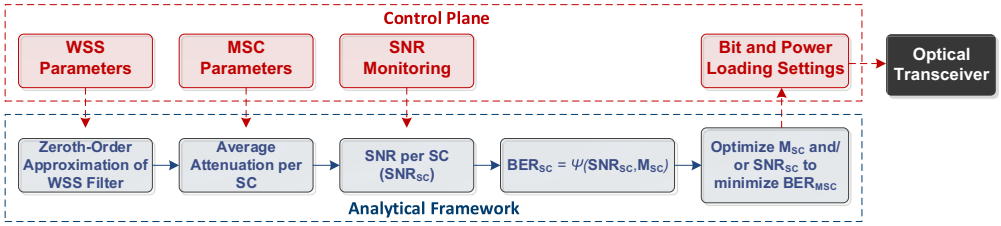

Fig. 2. Block diagram of the optimization and control process we propose based on the zeroth-order approximation for the WSS transfer function.

Making use of these input parameters obtained from the control plane, we may now utilize the analytical framework provided by expressions (4)–(8) in order to optimize the MSC parameters (i.e. the vectors of modulation orders and power-ratios per subcarrier, $\mathbf{M_{SC}}$ and $\mathbf{PR_{SC}}$) through bit- and/or power-loading, with the aim to minimize the global MSC BER, BER_{MSC}. We can then mathematically define the power-loading (PL) strategy as the following optimization over $\mathbf{PR_{SC}}$,

$$\mathbf{PR_{SC,PL}} = \underset{\mathbf{PR_{SC}}\in\mathbb{R}}{\operatorname{argmin}} \left[\mathrm{BER_{MSC}} \left(\mathrm{SNR_{MSC}} - 10\log_{10}(\hat{\mathbf{L}}_{\mathbf{SC}}) + \mathbf{PR_{SC}}, \mathbf{M_{SC}} \right) \right], \tag{9}$$

where $\mathbf{PR_{SC,PL}}$ is the vector optimized power-ratios per SC. Conversely, the bit-loading (BL) strategy can be defined as,

$$\mathbf{M_{SC,BL}} = \underset{M_{SC_n}=2^k,\ k\in\mathbb{I}}{\operatorname{argmin}} \left[\mathrm{BER_{MSC}} \left(\mathbf{SNR_{SC}}, \mathbf{M_{SC}} \right) \right], \tag{10}$$

where $\mathbf{M_{SC,BL}}$ is the vector of optimized set of constellation orders per SC. Finally, the bit-and-power-loading (BPL) strategy can be defined as the joint optimization of both $\mathbf{PR_{SC}}$ and $\mathbf{M_{SC}}$,

$$\left[\mathbf{M_{SC,BPL}}, \mathbf{PR_{SC,BPL}}\right] = \underset{\substack{\mathbf{PR_{SC}}\in\mathbb{R} \\ M_{SC_n}=2^k,\ k\in\mathbb{I}}}{\operatorname{argmin}} \left[\mathrm{BER_{MSC}} \left(\mathrm{SNR_{MSC}} - 10\log_{10}(\hat{\mathbf{L}}_{\mathbf{SC}}) + \mathbf{PR_{SC}}, \mathbf{M_{SC}} \right) \right]. \tag{11}$$

Most importantly, it is worth noting that using the analytical framework defined by expressions (1)-(11) the entire PL, BP and BPL processes are fully blind, in the sense that they do not require any feedback channel from the receiver. In addition, the zeroth-order approximation is also agnostic to the analytical formulation of the WSS transfer function, and therefore the same approach can be utilized for any other WSS formulations or even actual measurements of its optical transfer function.

It is also worth referring that the BER-based approach of expressions (7)–(11) is most adequate for hard-decision FEC coding, where pre-FEC BER can be utilized as an optimum metric. Instead, for SD-FEC coding it has been shown that the pre-FEC BER is actually modulation format dependent [19]. In those cases, expressions (7)–(11) should be reformulated in order to replace BER by generalized mutual information (GMI) as a performance metric. However, a fully-analytical GMI-based framework might not be feasible due to the absence of a closed-form analytical expression of GMI as a function of SNR.

Optics EXPRESS

3. Simulation assessment

To verify if the theoretical framework introduced in the previous section can be used for fast offline evaluation of WSS-induced performance degradation, a comprehensive simulation campaign has been carried out. Assuming ROADMs are placed along a link with periodical amplification, to perform simulations we considered two different emulations of ASE noise insertion: i) lumped noise, in which all the noise along the link is added in front of the receiver, and ii) equally distributed noise, in which the noise along link is equally split and added before each WSS.

3.1. Simulation parameters

The simulated system is a 200 Gb/s fixed rate system transmitting at 32 GBaud raw overall symbol-rate and implementing soft-decision forward error correction (SD-FEC) with $2.4 \cdot 10^{-2}$ maximum pre-FEC BER, as typically required by SD-FEC algorithms with 20% overhead [20]. As previously mentioned in Section 2, it is important to recall the modulation format dependency of pre-FEC BER with SD-FEC. Nevertheless, for relatively small FEC overheads and using modulation formats of similar order, this effect is expected to produce only small deviations of 0.1–0.2 dB on the overall required SNR of the MSC signal (see Fig. 3(a) of [19]).

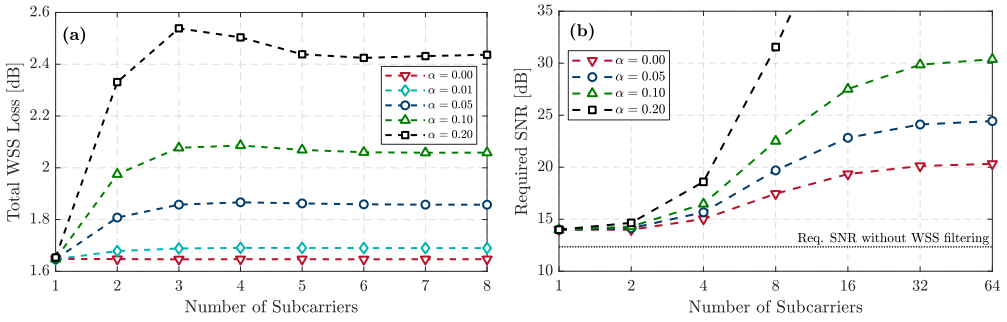

Fig. 3. Impact of the number of subcarriers on (a) the total WSS-induced loss and (b) the required SNR, without applying any bit and/or power-loading strategy. The simulated optical filtering corresponds to 8 cascaded WSSs.

Thanks to FDHMF, the target 200 Gb/s bit-rate can be achieved through the combination of different modulation formats. To compensate for ISI, we optionally consider a data-aided least mean squares (LMS) adaptive equalizer with an optimized number of taps. We consider different number of SCs (1, 2, 4, 8 and 16) and for all of them we analyze the evolution of the required SNR with respect to the increasing number of cascaded WSSs. Moverover, we perform the optimization of power-ratios and constellation orders for each SC, resorting to the PL, BL and BPL strategies. In order to assess the accuracy of the analytical framework, we also perform extensive Monte-Carlo simulations with BER counting, sweeping the parameters for bit and/or power-loading over a wide range, thereby finding the optimum settings by brute-force and comparing with the values obtained from the analytical expressions (9)–(11).

3.2. MSC performance without neither bit nor power loading

Before proceeding with the bit and/or power-loading optimization, let us start the simulation analysis by studying the impact of WSS-induced optical filtering on a standard MSC signal, based on the use of flat power and same modulation across all subcarriers. To that end, in Fig. 3 we consider an exemplary case of 8 cascaded WSS filters while sweeping the total number of subcarriers.

First, in Fig. 3(a) we address the total power loss induced by the cascaded WSS filters, applying expression (2). Here we can observe the key role played by pulse shaping in MSC signals. When

Optics EXPRESS

ideal Nyquist pulse shaping ($\alpha = 0$) is employed, the WSS-induced loss is independent of the number of subcarriers. However, as the roll-off increases, MSC signals tend to suffer from an additional loss. Although the spectral occupation of single-carrier and MSC signals is still exactly the same, $(1 + \alpha)R_s$, the usage of practical non-zero roll-off factors results in pushing the lateral MSC subcarriers towards the edges of the WSS filter, thereby resulting in an increased overall attenuation. For that reason, the choice of a low roll-off factor is of utmost importance for MSC design. For the remaining of this paper, we will consider a roll-off factor $\alpha = 0.05$, which guarantees a minor power-loss penalty.

Complementary to the baseline power-loss analysis, in Fig. 3(b) we also study the impact of WSS filtering on the required SNR of an MSC signal without any bit and/or power loading. The required SNR is analytically calculated from the BERs obtained by expression (8) for a wide range of $\mathrm{SNR_{MSC}}$ values. The first key conclusion to be taken from Fig. 3(b) is that MSC tends to yield an implementation penalty even for perfectly Nyquist-spaced subcarriers ($\alpha = 0$). Although counter-intuitive, this result can be easily justified by the ISI-free nature of the considered WSS approximation together with the fact that BER is a strictly convex function of SNR, i.e. $\Psi\left(\kappa\,\mathrm{SNR}_1 + (1-\kappa)\,\mathrm{SNR}_2\right) < \kappa\,\Psi\left(\mathrm{SNR}_1\right) + (1-\kappa)\,\Psi\left(\mathrm{SNR}_2\right)$. Provided that the same average loss is kept regardless of the number of subcarriers (which is true for $\alpha = 0$), i.e. $\mathrm{SNR_{MSC}}$ is fixed for the same WSS transfer function, then the convexity of the $\Psi(\cdot)$ function forces that,

$$\Psi\left(\mathrm{SNR_{MSC}}\right) < \frac{1}{N_{\mathrm{SC}}} \sum_{k=1}^{N_{\mathrm{SC}}} \Psi\left(\mathrm{SNR_{SC}}_k\right), \tag{12}$$

where $\mathrm{SNR_{MSC}} = \frac{1}{N_{\mathrm{SC}}} \sum_{k=1}^{N_{\mathrm{SC}}} \mathrm{SNR_{SC}}_k$. The immediate consequence of this inequality is that, *in the absence of ISI*, the overall BER of the MSC signal, $\mathrm{BER_{MSC}}$, as given by expression (8), is minimized for a single-carrier signal. While it is not commonly found in the literature, this is a fundamental result that should always be taken into consideration: in the absence of ISI, or considering perfect and ideal (without noise enhancement) ISI compensation at the receiver, the use of more subcarriers for signal modulation actually causes an increasing implementation penalty. However, in practical terms, the SNR loss created by WSS-induced optical filtering always comes together with an important ISI contribution. In that case, the increased impact of ISI on a single-carrier signal may overcome the underlying penalty of splitting the signal into subcarrier components, as we will demonstrate in the following. Another important consequence of the balance between these two opposite effects is that for each system there must be an optimum number of subcarriers that minimizes the overall BER. Also in Fig. 3(b) we can observe that increasing the roll-off factor results in further performance degradation. In addition to inherently degrading the required SNR, the increasing power-loss with N_{SC} (as previously shown in Fig. 3(a)) also enhances the imbalance between subcarrier BERs, which in turn increases the penalty associated with the convexity of the BER function.

This rather pessimistic preliminary analysis of baseline MSC performance clearly shows that transmitter-side MSC optimization is a key requirement to make it an advantageous signal design option for optical networking scenarios with strong WSS-induced filtering. This will be the main argument for the following sections, in which we will recur to optimized bit and/or power loading driven by the analytical framework presented in section 2.

3.3. MSC performance with optimized bit and/or power loading: 8 subcarriers

We start our simulation analysis by considering an 8×4 GBaud signal [10], which is compared to a 16QAM 32 GBaud single-carrier signal. For the MSC signal we consider four different options: i) same modulation (16QAM) and same (flat) power for all SCs, ii) PL, iii) BL, and iv) BPL. Fig. 4 shows a complete and compact summary of the obtained simulation results and it is organized in the following way. The two plots on top (Figs. 4(a) and 4(b)) show the

Optics EXPRESS

required SNR for an increasing number of cascaded WSSs in case of lumped noise and more realistic (non-approximated) WSS filtering, where the one on the left does not consider adaptive equalization, while the one on the right does. The same organization applies for Figs. 4(c) and 4(d) in the middle row, in which the noise is now equally distributed along the link. In Figs. 4(a)–4(d), BL and/or PL results are obtained performing a brute-force optimization. For BL, after the determination of all the FDHMF sets of constellation orders yielding 200G net capacity, the set providing the lowest required SNR was selected. Whilst, for PL the power-ratio per subcarrier was optimized using *fminsearch* Matlab function. Finally, the theoretical predictions provided by expressions (1)–(11) (analytical framework) are shown in the bottom row in Fig. 4(e) and used in Fig. 4(f) to evaluate deviations of the simulation results implementing equalization in case of single-carrier and 8 SCs with BL and BPL.

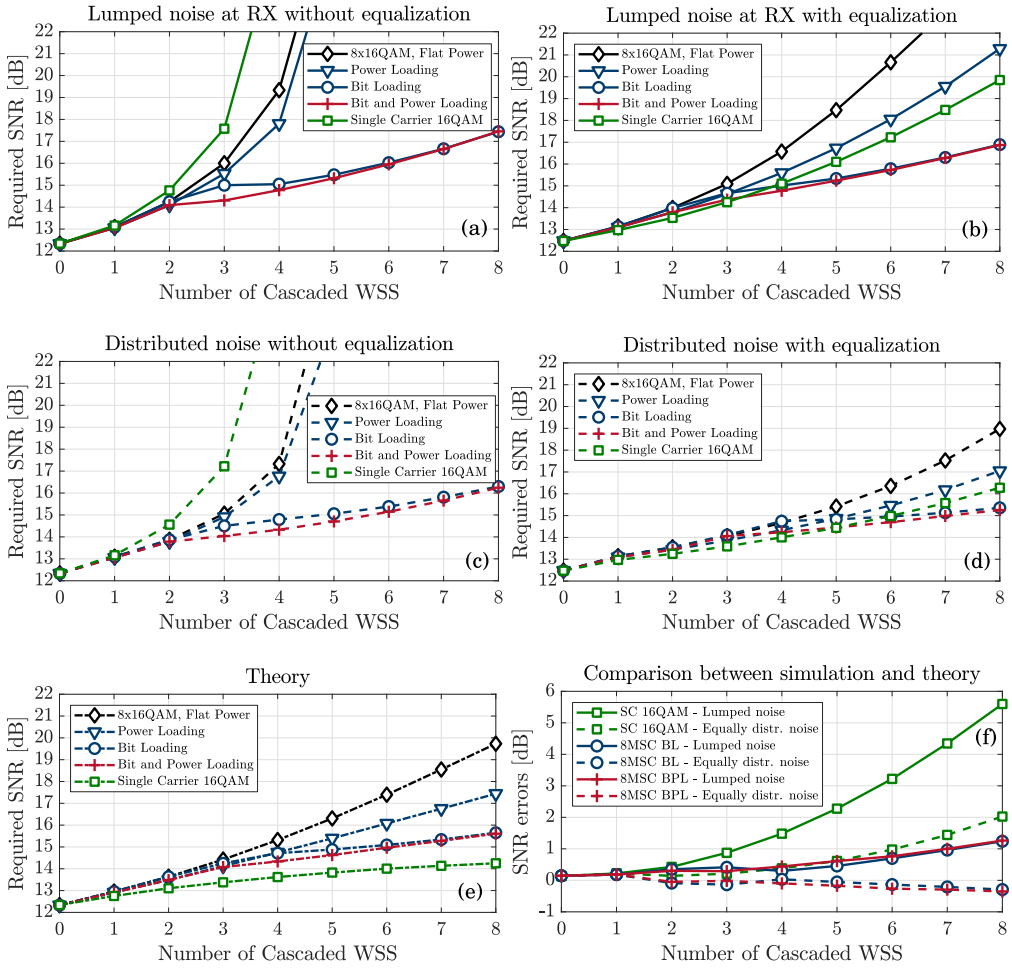

Fig. 4. Required SNR for an increasing number of cascaded WSSs in case of (a) lumped noise at the RX without equalization, (b) lumped noise at the RX with equalization, (c) equally distributed noise without equalization, (d) equally distributed noise with equalization. In (a)–(d), PL and/or BL curves are the result of a brute-force optimization. Then (e) theoretical required SNR for an increasing number of cascaded WSSs obtained using the analytical framework and (f) error deviation between the simulation and the theory only for the case with equalization.

Optics EXPRESS

In order to analyze the impact of ISI more in depth, we may compare the obtained results with and without adaptive equalizer at the receiver. Let us start by analyzing the results obtained with lumped noise added at the receiver, shown in Figs. 4(a) and 4(b). Here, we can see that the single-carrier performance is significantly affected by ISI, as its required SNR grows exponentially with the number of cascaded WSS when no equalization is applied at the receiver. In fact, we observe that the single-carrier signal behaves worse than the equivalent 8 SCs solution with fixed modulation and flat power, which already demonstrates the inherent increased resilience of MSC modulation towards WSS-induced ISI. Although the MSC performance can be slightly improved through PL, we can observe a major improvement through BL that is obviously maintained when applying the BPL. Moreover, it is remarkable to observe that after 8 cascaded WSSs the BL, and consequently the BPL, performance with and without adaptive equalization at the receiver only differs by approximately 0.5 dB. This shows that the BL strategy is very effective in mitigating filtering penalties, significantly alleviating the burden from the adaptive equalizer, up to the point of almost enabling its complete removal. As shown in Fig. 4(b), the use of an adaptive equalizer at the receiver significantly boosts the performance of the single-carrier signal. In fact, we can observe that the single-carrier 16QAM signal always behaves better that the corresponding MSC signal with fixed modulation and flat power. Even when PL is applied to the MSC signal, its performance is still slightly worse than its single-carrier counterpart. Once again, the advantage of using MSC modulation is only achievable through an adequate optimization of the constellations per subcarrier, i.e. through BL. In that case, the gain after 8 cascaded WSSs is of about 3 dB in required SNR. Note that, even if equalization provides a significant reduction of the required SNR, performances are always worse than predicted by theory. This is explained by the fact that, implementing equalization, not only the useful signal is enhanced, but also the noise.

Since the equally distributed noise scenario is more similar to a realistic case and the theory has been derived for the case of lumped noise at the receiver (worst case), it is important to analyze the error caused by this assumption. As expected, the simulation results plotted in Figs. 4(c) and 4(d) show that the performance with equally distributed noise are significantly improved: after 8 cascaded WSSs, the minimum required SNR with MSC and BL/BPL are about 2 dB lower in the distributed noise scenario. Nevertheless, we can observe that the general performance trends are very similar to those of a lumped noise system, namely in what regards the relative comparison between single-carrier and MSC with power- and bit-loading. Notably, the MSC gain (with BL) after 8 cascaded WSSs is now reduced to approximately 1 dB.

Finally, in Fig. 4(f) we directly compare the simulation results with those obtained from the theoretical framework derived in the previous section. As previously asserted, the theory is optimistic for the lumped noise scenario, as it considers perfect ISI removal at the receiver: this causes a steady increase of the SNR error with an increasing number of WSS filters. But if for MSC the error after 7 cascaded WSSs is limited to about 1 dB, for single-carrier it exceeds 4 dB confirming that this simple theory is not applicable to this case. The worst case lumped noise assumption contributes to a pessimist prediction but at the same time the theory does not take into account ISI. Remarkably, the accumulation of these two opposite sign errors bring the theoretical predictions to a very high-level of accuracy: less than 0.5 dB error after 8 cascaded WSSs.

After analyzing the overall required SNR, we now proceed to evaluate the optimization of modulation formats and the corresponding power-ratios per SC. Here we analyze the specific case of lumped noise and adaptive equalization, but similar results can be obtained in case of equally distributed noise. By performing brute-force PL and BPL, it is possible to check if the results obtained applying the analytical expressions (9)–(11) agree with the simulation results or if there exist more suitable modulation formats and power-ratios. Brute-force PL is applied over all the possible FDHMF constellation sets that provide a 200G net bit-rate. Then BL is performed by selecting the best FDHMF configurations that minimize the required SNR for each number of cascaded WSS filters. In Fig. 5, the three best FDHMF constellation sets, the brute-force

Optics EXPRESS

BPL (black dashed line) and the theoretical curve for BPL (red dashed line) are illustrated. The selected modulation formats per SC, which are symmetric with respect to the central SCs, are presented in Table 1 for both theory and brute-force optimization through simulation. From there we can see that for few WSSs (1 and 2), filtering effects are not significantly strong at the edge SCs, thus the transmitted modulation format is still 16QAM. Moving to a larger number of cascaded WSSs, lower modulation formats (QPSK) are allocated to edge SCs, while going towards the central SCs, the modulation cardinality increases (16QAM and 32QAM).

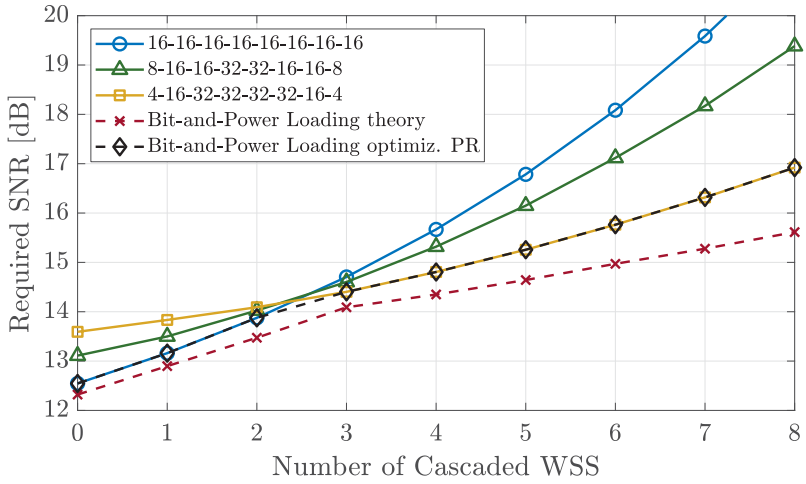

Fig. 5. Comparison of BPL based on theoretical PRs (red dashed line) and BPL based on brute-force optimized PRs (black dashed line) with equalization for an 8×4 GBaud MSC signal and lumped noise.

Table 1. Best FDHMF constellations for different number of cascaded WSSs respectively based on theory (on the left) and on brute-force BPL optimization (on the right) for a 8×4 GBaud signal in a lumped noise scenario.

	Theoretical BPL								Brute-Force BPL Optimization							
N_{WSS}	Modulation Format per Subcarrier								Modulation Format per Subcarrier							
0	16	16	16	16	16	16	16	16	16	16	16	16	16	16	16	16
1	16	16	16	16	16	16	16	16	16	16	16	16	16	16	16	16
2	16	16	16	16	16	16	16	16	16	16	16	16	16	16	16	16
3	4	16	32	32	32	32	16	4	4	16	32	32	32	32	16	4
4	4	16	32	32	32	32	16	4	4	16	32	32	32	32	16	4
5	4	16	32	32	32	32	16	4	4	16	32	32	32	32	16	4
6	4	16	32	32	32	32	16	4	4	16	32	32	32	32	16	4
7	4	16	32	32	32	32	16	4	4	16	32	32	32	32	16	4
8	4	16	32	32	32	32	16	4	4	16	32	32	32	32	16	4

As the modulation formats given by brute-force BPL are the same as those given by theory, also PR values are similar, which are shown in Fig. 6: analytical on the left and simulated on the right. This also justifies that, although there is an absolute difference between the theoretical predictions and simulation results (see red and black dashed curves in Fig. 5), the general dependence of

Optics EXPRESS

required SNR on the number of cascaded WSS filters actually follows very similar trends. In case of 1 and 2 cascaded WSSs, PRs at the edge SCs are higher in order to compensate for optical filtering. Instead, when crossing 3 cascaded WSSs we move to the constellation set [4 16 32 32 32 32 16 4], for which PRs are lower at the edge SCs and higher at the central SCs because higher order constellations requires increased $\mathbf{SNR_{SC}}$. While increasing the number of cascaded WSSs, PRs tend to recover the initial behavior, i.e. they increase at the edge and decrease in the center, still to mitigate optical filtering. From these results we can conclude that, for an 8×4 GBaud signal, the analytic evaluation and compensation of optical filtering along the link is a promising and fast alternative to classic extensive time-domain simulation campaigns. It is worth emphasizing that, while the full simulation scenario whose results are depicted in Figs. 4–6 required several days of intensive processing in dedicated server machines, the corresponding theoretical predictions can be obtained in just a few seconds.

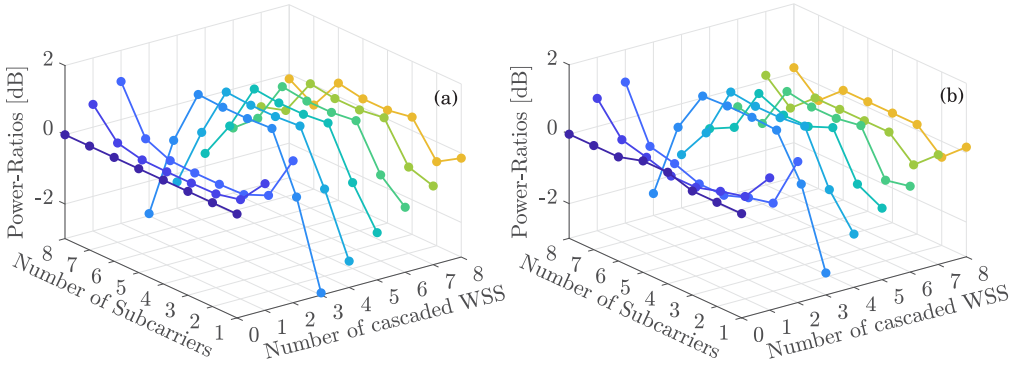

Fig. 6. (a) Theoretical PRs per subcarrier and (b) optimized PRs obtained from brute-force BPL for an 8×4 GBaud signal in a lumped noise scenario.

3.4. *On the optimum number of subcarriers*

With the aim to find the optimum number of subcarriers that yields maximum resilience towards WSS filtering, we repeat the previous study for 2×16 GBaud, 4×8 GBaud and 16×2 GBaud MSC signals as well. The results are summarized in Fig. 7. If no optimization strategy is implemented, i.e. in the case of fixed modulation and flat-power, increasing the number of cascaded WSSs, the use of MSC only starts to pay-off when more than 8 SCs are used, but the required SNR is still higher than the one required by the single-carrier modulation. This clearly shows that, without optimizing power-ratios and/or constellations per SC, MSC on its own is not effective in mitigating filtering penalties. We can also observe that, the use of standalone BL is much more effective in compensating filtering penalties than the corresponding use of standalone PL. Actually, the use of joint BPL only brings a small incremental benefit over BL. This is an important observation, as it significantly simplifies the FDHMF optimization process. In addition, maintaining a flat or nearly-flat power across SCs may also be beneficial in terms of nonlinear fiber propagation [8]. Finally, as expected due to the convexity of the $\Psi(\cdot)$ function, we can observe that the dependence of the required SNR on the number of SCs is non-monotonic, i.e. there exists an optimum N_{SC} that maximizes performance. For example, after 8 cascaded WSSs we observe an improvement of about 3 dB in required SNR when using the 8 subcarries optimized using the BPL (or BL) approach compared to the single-carrier case. Most importantly, the optimum number of SCs found in Fig. 7 is within the range of 8–16 SCs, corresponding to a symbol-rate per SC of 2–4 GBaud, which exactly matches the region of optimal symbol-rates that has been found to minimize the impact of fiber nonlinearities [7]. This suggests that MSC signals

Optics EXPRESS

can effectively combine the advantages of enhanced optical filtering resilience and nonlinear interference mitigation, which might be an important result for terrestrial metro optical networks.

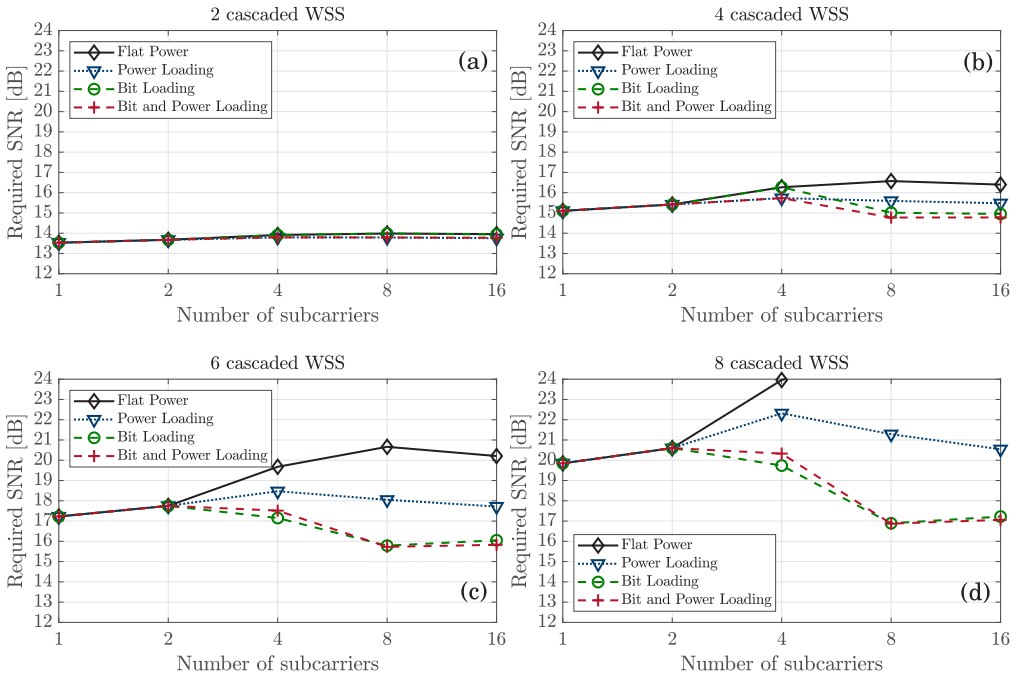

Fig. 7. Comparison among different power ratio strategies in terms of required SNR versus number of subcarriers for (a) 2, (b) 4, (c) 6 and (d) 8 cascaded WSSs.

4. Experimental validation

4.1. Experimental setup

After a comprehensive simulation study, we carried out an experimental validation considering the same system parameters: sweeping the number of SCs from 2 to 16 with a 200G rate constraint and considering SD-FEC with $2.4 \cdot 10^{-2}$ target BER. Making use of the theoretical formulation described in section 2, we perform BL, PL and BPL fully driven by the analytical expressions residing in the control plane of the system. This enables to set BL, PL and BPL *a priori*, without the need for any feedback from the receiver and avoiding to perform unfeasible brute-force optimization of experimental parameters. The experimental setup is depicted in Fig. 8 and it is the same used in [10]. It is an optical back-to-back (OB2B) setup with noise loading where we mimick the presence of cascaded WSSs through a WaveShaper (WS) programmable optical filter. At the transmitter side, signal samples are processed offline and then uploaded to the arbitrary waveform generator (AWG), which generates the analog electrical MSC signal at 64 GSamples/s. To reduce the performance impact of bandwidth limitation at the transmitter, it includes digital pre-emphasis. Each SC is shaped by a root-raised-cosine (RRC) with 0.05 roll-off factor. Then, a single-polarization IQ modulator (IQM), fed by an external cavity laser (ECL), optically up-converts the electrical signal. Polarization-multiplexing (PM) is emulated by inserting a delay of about 5 ns between polarizations, which is achieved by propagating the y-polarized signal component along a 1 m long piece of fiber. Afterwards, the two signal components are combined together through a polarization beam combiner (PBC). The ROADM effect, i.e. the optical filtering caused by cascaded WSSs (B = 37.5 GHz and B_{OTF} = 10.4 GHz),

Optics EXPRESS

is emulated by the WaveShaper that implements the transfer function of expression Eq. (1). The signal experimental traces obtained from an optical spectrum analyzer (OSA) are shown in Fig. 9.

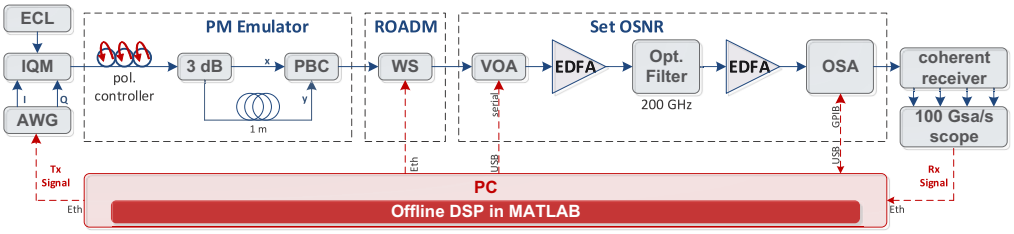

Fig. 8. Experimental setup for the optical back-to-back scenario with ROADM filtering emulation.

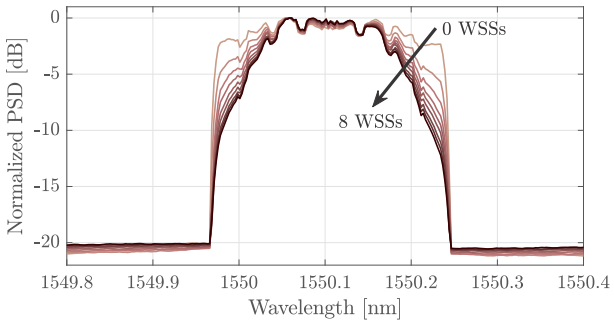

Fig. 9. Experimental traces obtained from the OSA for the emulation of a different number of cascaded ROADMs ($N_{\mathrm{WSS}} = 0 \ldots 8$).

A variable optical attenuator (VOA) and the first erbium-doped fiber amplifier (EDFA) are used to perform noise loading, needed to set the operating OSNR. A 200 GHz optical filter is placed to remove the out-of-band noise and the second EDFA guarantees a fixed optical power at the input of the coherent receiver. An OSA measuring a tapped signal after the second EDFA allows us to calculate the OSNR of operation. At the receiver side, after coherent detection, analog to digital conversion (ADC) of the signal is performed with a real-time oscilloscope (50 Gsample/s). Then, offline digital signal processing (DSP) is applied in Matlab. The data-aided DSP includes an initial constant modulus algorithm (CMA) based adaptive equalizer for pre-convergence with an optimized number of taps, followed by frequency offset removal and Viterbi & Viterbi phase estimation (101 taps). A second adaptive equalizer based on real-valued LMS is finally applied before symbol demapping and error counting. Before starting to measure the impact of ROADM filtering we have analyzed our MSC system in back-to-back condition in order to evaluate the implementation penalty. We found that, independently of both the number of subcarriers and the hybrid configuration, our experimental setup suffered a penalty of ~0.9 dB.

4.2. *Experimental results*

Experimental results are summarized in Fig. 10, a representation similar to Fig. 7, where the required SNR is shown as a function of number of SCs and number of cascaded WSSs (2, 4, 6 and 8). Directly comparing experimental and simulation results we find that, up to 4 cascaded WSSs, the required SNRs from simulations are always lower than the experimental values for all the considered strategies. This extra penalty (almost 2 dB for the single-carrier case) is due to our OB2B setup and in particular to other noise sources not included in the simulations.

Optics EXPRESS

Passing through more filters, experimental results tend to become slightly more optimistic than simulations. In the worst case (fixed modulation and flat power with 8 cascaded WSSs and more than 2 SCs), we get more than 3 dB penalty between simulation and experimental results. This is due to the technical limitations of the WaveShaper used in our experiments, which is not able to correctly emulate the transfer function of a very large number of cascaded WSSs, due to its limited frequency resolution. Nevertheless, the general trend on required SNR is analogous to the previously analyzed simulation results, with the best filtering tolerance being achieved with 8–16 SCs together with BL and BPL. The highest gain with respect to single-carrier (2 dB) is achieved for 8 cascaded WSSs. In contrast, in all the individual plots of Fig. 10, the solid black curve related to fixed modulation and flat power increases for an increasing number of cascaded WSSs and SCs, suggesting that single-carrier is still a better solution than simple MSC modulation. Therefore, the use of MSC should always be combined with BL, PL or BPL. One of the main differences regarding the simulation analysis of section 3 is the enhanced performance of the PL strategy, which might be related with the non-ideal frequency response of the optical transceivers: therefore, PL might not only be counteracting the WSS filtering, but inherently performing some pre-emphasis of the transceiver response.

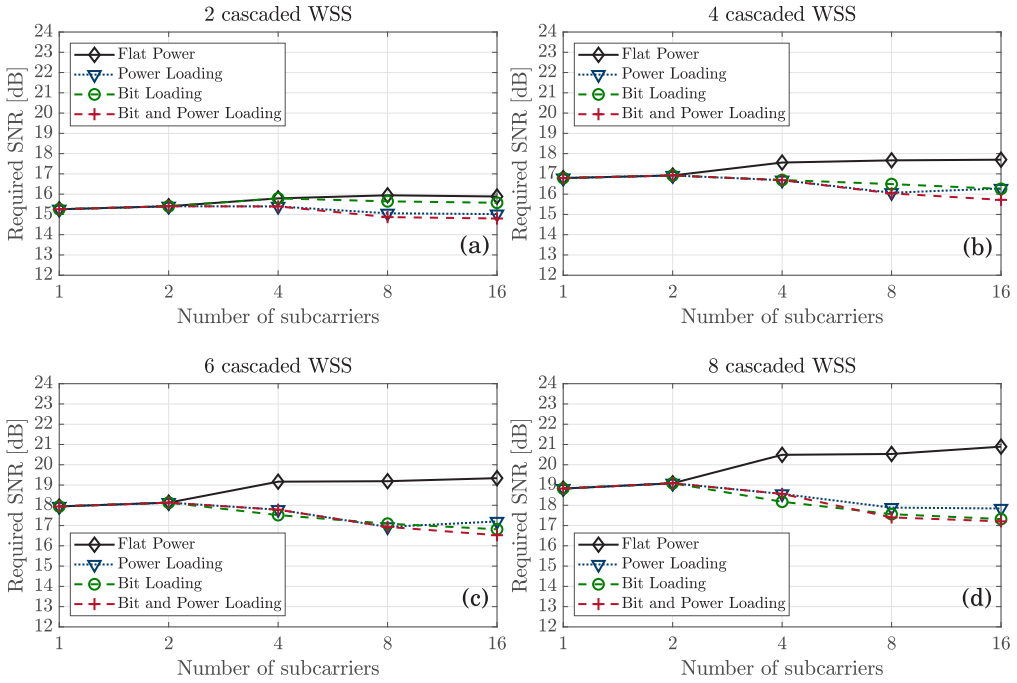

Fig. 10. Experimental required SNR versus number of subcarriers for (a) 2, (b) 4, (c) 6 and (d) 8 cascaded WSSs.

5. Conclusions

Employing a zeroth-order approximation of the well-known WSS transfer function, we have proposed a fully analytical framework for an accurate prediction of ROADM-induced filtering penalties in multi-subcarrier signals. This framework can be easily included in the control plane management of optical networks, enabling a real-time estimation of optimal BL, PL and BPL parameters only requiring basic knowledge of ROADM and signal modulation. Using optimized BL, PL and BPL driven by the control plane, we demonstrate both by simulations and transmission

Optics EXPRESS

experiments that MSC provides a better alternative to simple single-carrier modulation when the lightpath traverses several cascaded ROADMs. Coincidentally, we have also found that the typical symbol-rate per SC that optimizes performance under strong ROADM-induced optical filtering is within the same range as that required for optimal nonlinear mitigation through symbol-rate optimization: 2–4 GBaud. This shows that MSC modulation can be an interesting alternative not only for point-to-point long-haul transmission but also for optically routed network scenarios. The maximum gain in terms of required SNR obtained after 8 cascaded WSSs (4 ROADMs) was approximately ~2 dB, using an MSC signal composed of 8 SCs with BL directly provided by the control plane, i.e. without requiring any real-time feedback channel from the receiver. Finally, it is important to stress that, although the simulation and experimental results provided in this paper have been focused on a 200G system, the proposed analytical framework can be straightforwardly applied to any other combination of symbol-rates, frequency grids and WSS transfer functions. Indeed, it may be utilized for a fast evaluation of ROADM-induced penalties in a wide variety of scenarios, enabling to obtain a wider picture of achievable performances in optically routed networks.

Funding

Programa Operacional Temático Factores de Competitividade (CENTRO-01-0145-FEDER-022141, POCI-01-0145-FEDER-016432); European Regional Development Fund.

References

1. M. Benisha, R. T. Prabu, and D. V. Thulasi Bai, "Requirements and challenges of 5G cellular systems," in *International Conference on Advances in Electrical, Electronics, Information, Communication and Bio-Informatics*, (2016).
2. T. Zami, I. Fernandez de Jauregui Ruiz, A. Ghazisaeidi, and B. Lavigne, "Growing impact of optical filtering in future WDM networks," in *Optical Fiber Communication Conference (OFC)*, (2019).
3. L. Li, A. Abd El-Rahman, and J. Cartledge, "Effect of bandwidth narrowing due to cascaded wavelength elective switches on the generalized mutual information of probabilistically shaped 64-QAM systems," in *European Conference of Optical Communication (ECOC)*, (2018).
4. T. Rahman, A. Napoli, D. Rafique, B. Spinnler, M. Kuschnerov, I. Lobato, B. Clouet, M. Bohn, C. Okonkwo, and H. de Waardt, "On the mitigation of optical filtering penalties originating from ROADM cascade," IEEE Photonics Technol. Lett. **26**(2), 154–157 (2014).
5. M. Filer and S. Tibuleac, "Cascaded ROADM Tolerance of mQAM optical signals employing nyquist shaping," in *IEEE Photonics Conference*, (2014).
6. Q. Wang, Y. Yue, J. Yao, and J. Anderson, "Adaptive compensation of bandwidth narrowing effect for coherent in-phase quadrature transponder through finite impulse response filter," Appl. Sci. **9**(9), 1950 (2019).
7. P. Poggiolini, A. Nespola, Y. Jiang, G. Bosco, A. Carena, L. Bertignono, S. M. Bilal, S. Abrate, and F. Forghieri, "Analytical and experimental results on system maximum reach increase through symbol rate optimization," J. Lightwave Technol. **34**(8), 1872–1885 (2016).
8. F. P. Guiomar, L. Bertignono, A. Nespola, and A. Carena, "Frequency-domain hybrid modulation formats for high bit-rate flexibility and nonlinear robustness," J. Lightwave Technol. **36**(20), 4856–4870 (2018).
9. A. Kumpera, V. Dominic, A. Awadalla, L. Dardis, J. Rahn, S. Sanders, M. Mitchell, P. Mertz, G. Shartle, S. Jackson, S. Blakey, M. Sokar, D. Krause, H. Sun, K. Wu, and P. Cannon, "Real-time superchannel transmission over 10,500 km submarine link at 4.66 b/s/Hz spectral efficiency," Opt. Express **26**(12), 15039–15044 (2018).
10. F. P. Guiomar, A. Lorences-Riesgo, A. M. Rosa Brusin, D. F. Morillo, A. Carena, and P. P. Monteiro, "Reducing ROADM filtering penalties using subcarrier multiplexing with offline bit and power loading," in *European Conference of Optical Communication (ECOC)*, (2018).
11. F. P. Guiomar, R. Li, C. R. S. Fludger, A. Carena, and V. Curri, "Hybrid modulation formats enabling elastic fixed-grid optical networks," J. Opt. Commun. Netw. **8**(7), A92–A100 (2016).
12. M. Xiang, Q. Zhuge, X. Zhou, M. Qiu, F. Zhang, T. M. Hoang, M. Y. S. Sowailem, M. Tang, D. Liu, S. Fu, and D. V. Plant, "Filtering tolerant digital subcarrier multiplexing system with flexible bit and power loading," in *Optical Fiber Communications Conference and Exhibition (OFC)*, (2017).
13. M. Xiang, Q. Zhuge, M. Qiu, F. Zhang, X. Zhou, M. Tang, S. Fu, and D. V. Plant, "Multi-subcarrier flexible bit-loading enable capacity improvement in meshed optical networks with cascaded ROADMs," Opt. Express **25**(21), 25046–25058 (2017).
14. E. Giacoumidis, X. Q. Jin, A. Tsokanos, and J. M. Tang, "Statistical performance comparisons of optical ofdm adaptive loading algorithms in multimode fiber-based transmission systems," IEEE Photonics J. **2**(6), 1051–1059 (2010).

Optics EXPRESS

15. T. A. Strasser and J. L. Wagener, "Wavelength-selective switches for ROADM applications," IEEE J. Sel. Top. Quantum Electron. **16**(5), 1150–1157 (2010).
16. C. Pulikkaseril, L. A. Stewart, M. A. F. Roelens, G. W. Baxter, S. Poole, and S. Frisken, "Spectral modeling of channel band shapes in wavelength selective switches," Opt. Express **19**(9), 8458–8470 (2011).
17. P. Vitthaladevuni and M.-S. Alouini, "A closed-form expression for the exact BER of generalized PAM and QAM constellations," IEEE Trans. Commun. **52**(5), 698–700 (2004).
18. P. Vitthaladevuni, M.-S. Alouini, and J. Kieffer, "Exact BER computation for cross QAM constellations," IEEE Trans. Wireless Commun. **4**(6), 3039–3050 (2005).
19. A. Alvarado, E. Agrell, D. Lavery, R. Maher, and P. Bayvel, "Replacing the soft-decision FEC limit paradigm in the design of optical communication systems," J. Lightwave Technol. **33**(20), 4338–4352 (2015).
20. G. Tzimpragos, C. Kachris, I. B. Djordjevic, M. Cvijetic, D. Soudris, and I. Tomkos, "A survey on FEC codes for 100 G and beyond optical networks," IEEE Commun. Surv. Tutorials **18**(1), 209–221 (2016).